Space-Time Hexahedral Finite Element Methods for Parabolic Evolution Problems

Ulrich Langer and Andreas Schafelner

1 Introduction

We consider the parabolic initial-boundary value problem (IBVP), find u such that

$$\partial_t u - \mathrm{div}_x(\alpha \nabla_x u) = f \text{ in } Q,\ u = u_D := 0 \text{ on } \Sigma,\ u = u_0 := 0 \text{ on } \Sigma_0, \qquad (1)$$

as a model problem typically arising in heat conduction and diffusion, where $Q = \Omega\times(0,T)$, $\Sigma = \partial\Omega\times(0,T)$, and $\Sigma_0 = \Omega\times\{0\}$. The spatial domain $\Omega \subset \mathbb{R}^d$, $d = 1, 2$, is assumed to be bounded and Lipschitz, $T > 0$ is the terminal time, $f \in L_2(Q)$ denotes a given source, and $\alpha \in L_\infty(Q)$ is a given uniformly positive (almost everywhere) coefficient that may discontinuously depend on the spatial variable $x = (x_1, \ldots, x_d)$ and the time variable t, but $\alpha(x,t)$ should be of bounded variation in t for almost all $x \in \Omega$. Then there is a unique weak solution $u \in V_0 := \{v \in L_2(0,T;H^1_0(\Omega)) : \partial_t u \in L_2(0,T;H^{-1}(\Omega)), v = 0 \text{ on } \Sigma_0\}$ of the IBVP (1); see, e.g., [4, 14]. Moreover, $\partial_t u$ and $Lu := -\mathrm{div}_x(\alpha \nabla_x u)$ belong to $L_2(Q)$; see [3]. The latter property is called maximal parabolic regularity. In this case, the parabolic partial differential equation $\partial_t u - \mathrm{div}_x(\alpha \nabla_x u) = f$ holds in $L_2(Q)$. This remains even valid for inhomogeneous initial conditions $u_0 \in H^1_0(\Omega)$.

Time-stepping methods in combination with some spatial discretization method like the finite element method (FEM) are still the standard approach to the numerical solution of IBVPs like (1); see, e.g., [16]. This time-stepping approach as well as the more recent discontinuous Galerkin, or discontinuous Petrov-Galerkin methods based on time slices or slabs are in principle sequential. The sequential nature of these methods hampers the full space-time adaptivity and parallelization; but

Ulrich Langer
Institute for Computational Mathematics, Johannes Kepler University, Altenbergerstr. 69, 4040 Linz, Austria, e-mail: ulanger@numa.uni-linz.ac.at

Andreas Schafelner
Doctoral Program "Computational Mathematics", Johannes Kepler University, Altenbergerstr. 69, 4040 Linz, Austria, e-mail: andreas.schafelner@dk-compmath.jku.at

see the overview paper [5] for parallel-in-time methods. Space-time finite element methods on fully unstructured decomposition of the space-time cylinder Q avoid these bottlenecks; see [15] for an overview of such kind of space-time methods.

In this paper, we follow our preceding papers [9, 11, 10], and construct locally stabilized, conforming space-time finite element schemes for solving the IBVP (1), but on hexahedral meshes that are more suited for anisotropic refinement than simplicial meshes used in [9, 11, 10]. We mention that SUPG/SD and Galerkin/least-squares stabilizations of time-slice finite element schemes for solving transient problems were already used in early papers; see, e.g., [8] and [6]. Section 2 recalls the construction of locally stabilized space-time finite element schemes, the properties of the corresponding discrete bilinear form, and the a priori discretization error estimates from [9, 11, 10]. In Section 3, we derive new anisotropic a priori discretization estimates for hexahedral tensor-product meshes, and we provide anisotropic adaptive mesh refinement strategies that are based on a posteriori error estimates, anisotropy indicators, and anisotropic adaptive mesh refinement using hanging nodes. In Section 4, we present and discuss numerical results for an example where a singularity occurs in the spatial gradient of the solution. The large-scale system of space-time finite element equations is always solved by means of the Flexible Generalized Minimal Residual (FGMRES) method preconditioned by space-time algebraic multigrid.

2 Space-time finite element methods

In this section, we will briefly describe the space-time finite element method based on localized time-upwind stabilizations; for details of the construction and analysis, we refer to our previous work [9, 11, 10]. Let $\mathcal{T}_h$ be a shape regular decomposition of the space-time cylinder Q, i.e., $\overline{Q} = \bigcup_{K \in \mathcal{T}_h} \overline{K}$, and $K \cap K' = \emptyset$ for all K and K' from $\mathcal{T}_h$ with $K \neq K'$; see, e.g., [2] for more details. Furthermore, we assume that α is piecewise smooth, and possible discontinuities are aligned with the triangulation as usual. On the basis of the triangulation $\mathcal{T}_h$, we define the space-time finite element space

$$V_{0h} = \{v \in C(\overline{Q}) : v(x_K(\cdot)) \in \mathcal{P}_p(\hat{K}),\ \forall K \in \mathcal{T}_h,\ v = 0 \text{ on } \overline{\Sigma} \cup \overline{\Sigma}_0\},$$

where $x_K(\cdot)$ denotes the map from the reference element $\hat{K}$ to the finite element $K \in \mathcal{T}_h$, and $\mathcal{P}_p(\hat{K})$ is either the space of polynomials of at most degree p on the reference element $\hat{K}$, or the space of polynomials of degree p in each variable on $\hat{K}$, for simplicial or tensor-product decompositions, respectively. Since we are in the maximal parabolic regularity setting, the parabolic Partial Differential Equation (PDE) is valid in $L_2(Q)$. Multiplying the PDE (1), restricted to $K \in \mathcal{T}_h$, by a locally scaled upwind test function $v_{h,K}(x,t) := v_h(x,t) + \theta_K h_K \partial_t v_h(x,t),\ v_h \in V_{0h}$, integrating over K, summing over all elements, applying integration by parts, and incorporating the Dirichlet boundary conditions, we obtain the variational consistency identity

$$a_h(u, v_h) = \ell_h(v_h), \quad \forall v_h \in V_{0h}, \tag{2}$$

with the mesh-dependent bilinear form

$$\begin{aligned} a_h(u, v_h) = \sum_{K \in \mathcal{T}_h} \int_K \big[& \partial_t u v_h + \theta_K h_K \partial_t u \partial_t v_h \\ & + \alpha \nabla_x u \cdot \nabla_x v_h - \theta_K h_K \mathrm{div}_x(\alpha \nabla_x u) \partial_t v_h \big] \mathrm{d}K, \end{aligned} \tag{3}$$

and the mesh-dependent linear form

$$\ell_h(v_h) = \sum_{K \in \mathcal{T}_h} \int_K \big[f v_h + \theta_K h_K f \partial_t v_h \big] \mathrm{d}K.$$

Now we apply the Galerkin principle, i.e., we look for a finite element approximation $u_h \in V_{0h}$ to u such that

$$a_h(u_h, v_h) = \ell_h(v_h), \quad \forall v_h \in V_{0h}. \tag{4}$$

Using Galerkin orthogonality (subtracting (4) from (2)), and coercivity and extended boundedness of the bilinear form (3), we can show the following Céa-like best approximation estimate; see [9, 11, 10] for the proofs.

Theorem 1 *Let $u \in H_0^{L,1}(Q) := \{v \in V_0 \cap H^1(Q) : Lv := -\mathrm{div}_x(\alpha \nabla_x v) \in L_2(Q)\}$ and $u_h \in V_{0h}$ be the solutions of the parabolic IBVP* (1) *and the space-time finite element scheme* (4)*, respectively. Then the discretization error estimate*

$$\|u - u_h\|_h \leq \inf_{v_h \in V_{0h}} \left(\|u - v_h\|_h + \frac{\mu_b}{\mu_c} \|u - v_h\|_{h,*} \right) \tag{5}$$

is valid provided that $\theta_K = O(h_K)$ is sufficiently small, where

$$\begin{aligned} \|v\|_h^2 &= \frac{1}{2} \|v(\cdot, T)\|_{L_2(\Omega)}^2 + \sum_{K \in \mathcal{T}_h} \Big[\theta_K h_K \|\partial_t v\|_{L_2(K)}^2 + \|\alpha^{1/2} \nabla_x v\|_{L_2(K)}^2 \Big], \\ \|v\|_{h,*}^2 &= \|v\|_h^2 + \sum_{K \in \mathcal{T}_h} \Big[(\theta_K h_K)^{-1} \|v\|_{L_2(K)}^2 + \theta_K h_K \|\mathrm{div}_x(\alpha \nabla_x v)\|_{L_2(K)}^2 \Big], \end{aligned}$$

and μ_c and μ_b are the coercivity and extended boundedness constants of the bilinear form (3)*, respectively.*

The best-approximation error estimate (5) now leads to convergence rate estimates under additional regularity assumptions. If the solution u of (1) belongs to $H_0^{L,1}(Q) \cap H^l(Q)$, $l > 1$, then $\|u - u_h\|_h \leq c(u) h^{s-1}$, where $s = \min\{l, p+1\}$, $h = \min_{K \in \mathcal{T}_h} h_K$, $c(u)$ depends on the regularity of u. We refer the reader to [9, Theorem 13.3] and [11, Theorem 3] for the proof of more detailed estimates in terms of the local mesh-sizes h_K and the local regularity of the solution u.

3 Anisotropic a priori and a posteriori error estimates

The convergence rate estimates presented at the end of the previous section consider only isotropic finite elements, but in many applications the solution u evolves differently with respect to time and space directions. So, we should permit anisotropic finite elements with different mesh sizes in different directions. This raises the question whether we can obtain (localized) a priori estimates that are explicit in spatial and temporal mesh sizes as well as in spatial and temporal regularity assumptions imposed on the solution u. We refer to [1] for a comprehensive summary of anisotropic finite elements. For the remainder of this section, we will now assume that K is a *brick element* (hexahedral element for the case $d = 2$), i.e., the edges of K are parallel to the coordinate axes. Moreover, we assume that $u \in H_0^{L,1}(Q) \cap H^m(Q) \cap H^l(\mathcal{T}_h)$, $m, l \in \mathbb{N}$ with $m > (d+1)/2$ and $l > d/2+2$. Let $h_{K,i} = \max\{|x_i - x_i'| : x, x' \in \overline{K}\}$, and let $h_{K,x} = \max_{i=1,\dots,d} h_{K,i} \geq h_{K,i} \geq c h_{K,x}$, and $h_{K,t} = h_{K,d+1}$. Now we replace h_K by $h_{K,x}$ at all places in Sect. 2. Furthermore, let $e_h = u - I_h u$ and $s = \min\{l, p+1\}$, where I_h is the Lagrange interpolation operator, and p is the polynomial degree of the finite element shape functions in every coordinate direction. Using the anisotropic interpolation error estimates from [1], we get

$$\|e_h\|^2_{L_2(K)} \leq c \left(\sum_{j=1}^{d} h_{K,j}^{2s} \|\partial_{x_j}^s u\|^2_{L_2(K)} + h_{K,t}^{2s} \|\partial_t^s u\|^2_{L_2(K)} \right),$$

$$\|\partial_{x_i}(e_h)\|^2_{L_2(K)} \leq c \left(\sum_{j=1}^{d} h_{K,j}^{2(s-1)} \|\partial_{x_i} \partial_{x_j}^{(s-1)} u\|^2_{L_2(K)} + h_{K,t}^{2(s-1)} \|\partial_{x_i} \partial_t^{(s-1)} u\|^2_{L_2(K)} \right),$$

$$\|\partial^2_{x_i}(e_h)\|^2_{L_2(K)} \leq c \left(\sum_{j=1}^{d} h_{K,j}^{2(s-2)} \|\partial^2_{x_i} \partial_{x_j}^{(s-2)} u\|^2_{L_2(K)} + h_{K,t}^{2(s-2)} \|\partial^2_{x_i} \partial_t^{(s-2)} u\|^2_{L_2(K)} \right),$$

for $i = 1, \dots, d+1$, where c denotes generic positive constants. In particular, we use [1, Thm. 2.7] for $d = 1$, and [1, Thm. 2.10] for $d = 2$. These estimates of the interpolation error and its derivatives immediately lead to the corresponding interpolation error estimates with respect to the norms $\|\cdot\|_h$ and $\|\cdot\|_{h,*}$. Now let $\mathcal{T}_h$ be a decomposition of Q into brick elements. Then we can derive the anisotropic interpolation error estimates

$$\|u - I_h u\|_h \leq \left(\sum_{K \in \mathcal{T}_h} h_{K,x}^{2(s-1)} \mathfrak{c}_1(u,K) + h_{K,t}^{2(s-1)} \mathfrak{c}_2(u,K) \right)^{1/2}, \tag{6}$$

$$\|u - I_h u\|_{h,*} \leq \left(\sum_{K \in \mathcal{T}_h} h_{K,x}^{2(s-1)} \mathfrak{c}_{1,*}(u,K) + h_{K,t}^{2(s-1)} \mathfrak{c}_{2,*}(u,K) \right)^{1/2}, \tag{7}$$

where $s = \min\{l, p+1\}$, and $\mathfrak{c}_1(u,K)$, $\mathfrak{c}_2(u,K)$, $\mathfrak{c}_{1,*}(u,K)$ and $\mathfrak{c}_{2,*}(u,K)$ can easily be computed from the interpolation error estimates given above. Here, $\mathfrak{c}_1(u,K)$,

$\mathfrak{c}_2(u,K)$, and $\mathfrak{c}_{1,*}(u,K)$ do not depend on the aspect ratio of the spatial and temporal mesh-sizes, whereas $\mathfrak{c}_{2,*}(u,K)$ depends on $h_{K,x}/h_{K,t}$ and $h_{K,t}/h_{K,x}$ quadratically. Combining the interpolation error estimates (6) and (7) with the best approximation estimate (5), where h_K must be replaced by $h_{K,x}$ in the definition of the norms, we can immediately derive an a priori discretization error estimate.

Theorem 2 *Let the best approximation estimate* (5) *hold, and let the anisotropic interpolation error estimates* (6) *and* (7) *be fulfilled. Then the anisotropic a priori discretization error estimate*

$$\|u-u_h\|_h \leq \left(\sum_{K\in\mathcal{T}_h} h_{K,x}^{2(s-1)} \mathfrak{C}_1(u,K) + h_{K,t}^{2(s-1)} \mathfrak{C}_2(u,K) \right)^{1/2},$$

is valid, where $s = \min\{l, p+1\}$*, and* $\mathfrak{C}_1(u,K)$ *and* $\mathfrak{C}_2(u,K)$ *can be computed from* (6) *and* (7)*.*

In the computational practice, we would like to replace the uniform mesh refinement by adaptive space-time mesh refinement that takes care of possible anisotropic features of the solution in space and time. Here brick finite elements with hanging nodes, as implemented in MFEM (see next section), are especially suited. To drive anisotropic adaptive mesh refinement, we need a localizable a posteriori error estimator providing local error indicators, and an anisotropy indicator defining the refinement directions in each brick element $K \in \mathcal{T}_h$.

We use the functional a posteriori error estimators introduced by Repin; see his monograph [13, Sect. 9.3]. Repin proposed two error majorants $\mathfrak{M}_1$ and $\mathfrak{M}_2$ from which the local error indicators

$$\eta_{1,K}^2(u_h) = \frac{1}{\delta}\int_K (1+\beta)\big[|\mathbf{y}-\alpha\nabla_x u_h|^2 + \frac{1}{\beta}c_{F\Omega}^2 |f-\partial_t u_h + \operatorname{div}_x \mathbf{y}|^2\big]\mathrm{d}K \text{ and}$$

$$\begin{aligned}\eta_{2,K}^2(u_h) =& \frac{1}{\delta}\int_K (1+\beta)\big[|\mathbf{y}-\alpha\nabla_x u_h + \nabla_x\vartheta|^2 + \frac{c_{F\Omega}^2}{\beta}|f-\partial_t u_h - \partial_t\vartheta + \operatorname{div}_x\mathbf{y}|^2\big]\mathrm{d}K \\ &+ \gamma\|\vartheta(\cdot,T)\|_\Omega^2 + 2\int_K \big[\nabla_x u_h\cdot\nabla_x\vartheta + (\partial_t u_h - f)\vartheta\big]\mathrm{d}K\end{aligned}$$

can be derived for each element $K \in \mathcal{T}_h$, where $\mathbf{y} \in H(\operatorname{div}_x, Q)$ is an arbitrary approximation to the flux, $\vartheta \in H^1(Q)$ is also an arbitrary function, $\delta \in (0,2]$, $\beta > \mu$, $\mu \in (0,1)$, and $\gamma > 1$. The positive constant $c_{F\Omega}$ denotes the constant in the inequality $\|v\|_{L_2(Q)} \leq c_{F\Omega}\|\sqrt{\alpha}\nabla_x v\|_{L_2(Q)}$ for all $v \in L_2(0,T;H_0^1(\Omega))$, which is nothing but the Friedrichs constant for the spatial domain Ω in the case $\alpha = 1$. Both majorants provide a guaranteed upper bound for the errors

$$|\!|\!| u-u_h |\!|\!|_{(1,2-\delta)}^2 \leq \sum_{K\in\mathcal{T}_h} \eta_{1,K}^2(u_h) \quad \text{and} \quad |\!|\!| u-u_h |\!|\!|_{(1-\frac{1}{\gamma},2-\delta)}^2 \leq \sum_{K\in\mathcal{T}_h} \eta_{2,K}^2(u_h),$$

where $|\!|\!| v |\!|\!|_{(\epsilon,\kappa)}^2 := \kappa\|\sqrt{\alpha}\nabla_x v\|_{L_2(Q)}^2 + \epsilon\|v(\cdot,T)\|_{L_2(\Omega)}^2$. Once we have computed the local error indicators $\eta_K(u_h)$ for all elements $K \in \mathcal{T}_h$, we use *Dörfler marking* to

determine a set $\mathcal{M} \subseteq \mathcal{T}_h$ of elements that will be marked for refinement. The set $\mathcal{M}$ is of (almost) minimal cardinality such that

$$\sigma \sum_{K \in \mathcal{T}_h} \eta_K(u_h)^2 \leq \sum_{K \in \mathcal{M}} \eta_K(u_h)^2,$$

where $\sigma \in (0,1)$ is a bulk parameter. Let $\mathbf{E}_K \in \mathbb{R}^{d+1}$ with entries $E_i^{(K)}$, $i = 1, \ldots, d+1$, and $\chi \in (0,1)$. In order to determine how to subdivide a marked element, we use the following heuristic: for each $K \in \mathcal{M}$, subdivide K in direction x_i iff $E_i^{(K)} > \chi |\mathbf{E}_K|$. In particular, we choose

$$\left(E_i^{(K)}\right)^2 := \begin{cases} \int_K (y_i - \alpha\, \partial_{x_i} u_h)^2 \, \mathrm{d}K, & i \leq d, \\ \int_K (\mathbf{d}_{\mathbf{t}h} - \partial_t u_h)^2 \, \mathrm{d}K, & i = d+1, \end{cases}$$

as our local anisotropy vector $\mathbf{E}_K$, where $\mathbf{y}_h = (y_i)_{i=1}^d$, $\mathbf{d}_{\mathbf{t}h} = R_h(\partial_t u_h)$, and R_h is some nodal averaging operator like in a Zienkiewicz-Zhu approach.

4 Numerical Results

Now let $\{p^{(j)} : j = 1, \ldots, N_h\}$ be the finite element nodal basis of V_{0h}, i.e., $V_{0h} = \mathrm{span}\{p^{(1)}, \ldots, p^{(N_h)}\}$, where N_h is the number of all space-time unknowns (dofs). Then we can express the approximate solution u_h in terms of this basis, i.e., $u_h(x,t) = \sum_{j=1}^{N_h} u_j\, p^{(j)}(x,t)$. Inserting this representation into (4), and testing with $p^{(i)}$, we get the linear system $K_h \underline{u}_h = \underline{f}_h$ for determining the unknown coefficient vector $\underline{u}_h = (u_j)_{j=1,\ldots,N_h} \in \mathbb{R}^{N_h}$, where $K_h = (a_h(p^{(j)}, p^{(i)}))_{i,j=1,\ldots,N_h}$ and $\underline{f}_h = (\ell_h(p^{(i)}))_{i=1,\ldots,N_h}$. The system matrix K_h is non-symmetric, but positive definite due to the coercivity of the bilinear form $a_h(\cdot,\cdot)$. Thus, in order to obtain a numerical solution to the IBVP (1), we just need to solve one linear system of algebraic equations. This is always solved by means of the FGMRES method preconditioned by space-time algebraic multigrid (AMG). We use the finite element library MFEM [12] to implement our space-time finite element solver. The AMG preconditioner is realized via *BoomerAMG*, provided by the linear solver library *hypre* [7]. We start the linear solver with initial guess $\mathbf{0}$, and stop once the initial residual has been reduced by a factor of 10^{-8}. In order to accelerate the solver in case of adaptive refinements, we also employ *Nested Iterations*. Here, we interpolate the finite element approximation from the previous mesh to the current mesh, and use that as an initial guess for FGMRES. Moreover, we stop the linear solver earlier, e.g. once the residual is reduced by a factor of 10^{-2}. Furthermore, we will use the notation $h = N_h^{-1/(d+1)}$ to indicate the corresponding convergence rates.

Let $Q = \Omega \times (0,1)$, where $\Omega = (0,1)^2 \setminus \{(x_1, 0) \in \mathbb{R}^2 : 0 \leq x_1 < 1\}$ is a "slit domain" that is not Lipschitz. Moreover, we choose the constant diffusion coefficient $\alpha \equiv 1$, and the manufactured solution $u(r, \varphi, t) = t\, r^\lambda \sin(\lambda\varphi)$, where (r, φ) are

polar coordinates with respect to (x_1, x_2), and $\lambda = 0.5$[1]. The singularity leads to a reduced convergence rate $O(h^{0.5})$ for the polynomial degrees $p = 1, 2$; see the upper plots of Fig. 1.

In order to properly realize the adaptive refinement strategies, we need to choose appropriate $\mathbf{y}$ and ϑ. For the first majorant, we reconstruct an improved flux $\mathbf{y}_h^{(0)} = R_h(\nabla_x u_h)$, where R_h is a nodal averaging operator. We then improve this flux by applying a few CG steps to the minimization problem $\min_{\mathbf{y}} \mathfrak{M}_1$, obtaining the final flux $\mathbf{y}_h^{(1)}$ that is then used in the estimator. For the second majorant, we follow the same procedure, but right before postprocssing the flux, we first apply some CG iteration to another minimization problem $\min_{\vartheta} \mathfrak{M}_2$.

For linear finite elements, we observe at least optimal convergence rates for both error estimators. Anisotropic refinements, with the anisotropy parameter $\chi = 0.1$, manage to obtain a better constant than isotropic refinements; see Fig. 1 (upper left). For quadratic finite elements, anisotropic adaptive refinements, with $\chi = 0.15$, manage to recover the optimal rate of $O(h^2)$, while isotropic adaptive refinements result in a reduced rate of $O(h^{1.25})$; see Fig. 1 (upper right). The efficiency indices are rather stable for isotropic refinements, while some oscillations can be observed for anisotropic refinements; see Fig. 1 (lower right).

Acknowledgements This work was supported by the Austrian Science Fund (FWF) under grant W1214, project DK4.

References

1. Thomas Apel. *Anisotropic finite elements: Local estimates and applications*. Teubner, Stuttgart, 1999.
2. Philippe G. Ciarlet. *The Finite Element Method for Elliptic Problems*. North-Holland Publishing Co., Amsterdam-New York-Oxford, 1978.
3. Dominik Dier. Non-autonomous maximal regularity for forms of bounded variation. *J. Math. Anal. Appl.*, 425(1):33–54, 2015.
4. Lawrence C. Evans. *Partial differential equations*, volume 19 of *Graduate Studies in Mathematics*. American Mathematical Society, Providence, RI, second edition, 2010.
5. Martin J. Gander. 50 years of time parallel time integration. In *Multiple shooting and time domain decomposition methods*, volume 9 of *Contrib. Math. Comput. Sci.*, pages 69–113. Springer, Cham, 2015.
6. Thomas J. R. Hughes, Leopoldo P. Franca, and Gregory M. Hulbert. A new finite element formulation for computational fluid dynamics. VIII. The Galerkin/least-squares method for advective-diffusive equations. *Comput. Methods Appl. Mech. Engrg.*, 73(2):173–189, 1989.
7. hypre: High performance preconditioners. http://www.llnl.gov/casc/hypre.
8. Claes Johnson and Jukka Saranen. Streamline diffusion methods for the incompressible Euler and Navier-Stokes equations. *Math. Comp.*, 47(175):1–18, 1986.
9. Ulrich Langer, Martin Neumüller, and Andreas Schafelner. Space-time finite element methods for parabolic evolution problems with variable coefficients. In *Advanced finite element methods with applications. Selected papers from the 30th Chemnitz finite element symposium, St. Wolfgang/Strobl, Austria, September 25–27, 2017*, pages 247–275. Cham: Springer, 2019.

[1] `https://math.nist.gov/amr-benchmark/index.html`

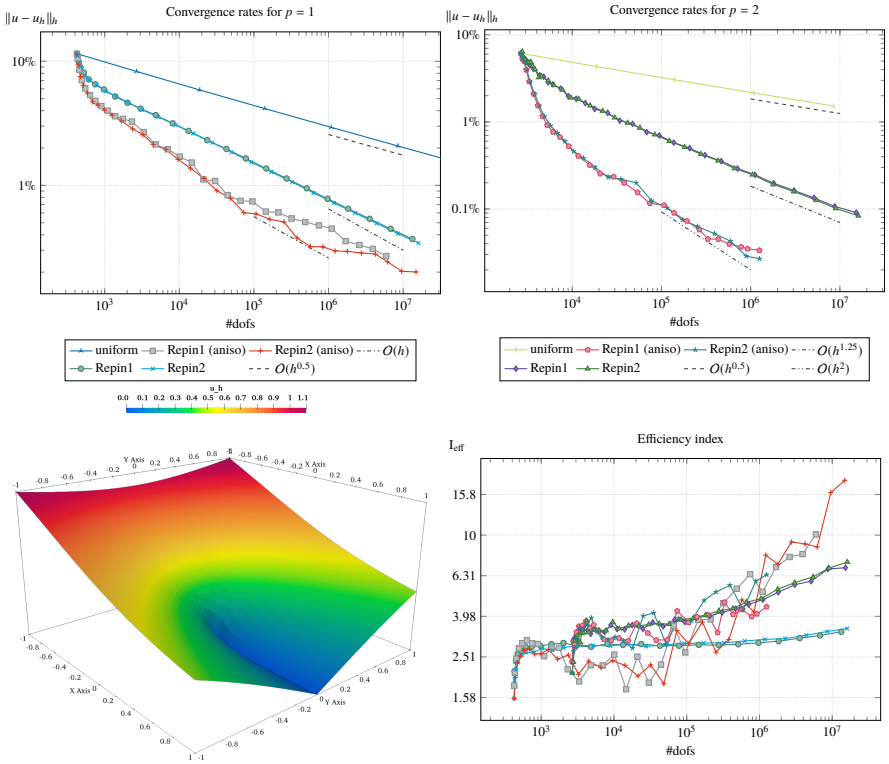

Fig. 1: Convergence rates for $p = 1$ (upper left); convergence rates for $p = 2$ (upper right); plot of $u(\cdot, \cdot, 1)$ (lower left); efficiency indices for $p = 1, 2$, with the respective styles from the upper plots (lower right).

10. Ulrich Langer and Andreas Schafelner. Adaptive space-time finite element methods for non-autonomous parabolic problems with distributional sources. *Comput. Methods Appl. Math.*, 20(4):677–693, 2020.
11. Ulrich Langer and Andreas Schafelner. Space-time finite element methods for parabolic initial-boundary value problems with non-smooth solutions. In *Large-scale scientific computing. 12th international conference, LSSC 2019, Sozopol, Bulgaria, June 10–14, 2019. Revised selected papers*, pages 593–600. Cham: Springer, 2020.
12. MFEM: Modular finite element methods library. mfem.org.
13. Sergey Repin. *A posteriori estimates for partial differential equations*, volume 4 of *Radon Series on Computational and Applied Mathematics*. Walter de Gruyter GmbH & Co. KG, Berlin, 2008.
14. Olaf Steinbach. Space-time finite element methods for parabolic problems. *Comput. Methods Appl. Math.*, 15(4):551–566, 2015.
15. Olaf Steinbach and Huidong Yang. Space-time finite element methods for parabolic evolution equations: discretization, a posteriori error estimation, adaptivity and solution. In *Space-time methods. Applications to partial differential equations*, pages 207–248. Berlin: De Gruyter, 2019.
16. Vidar Thomée. *Galerkin finite element methods for parabolic problems*, volume 25 of *Springer Series in Computational Mathematics*. Springer-Verlag, Berlin, second edition, 2006.